





- 30 1. The time-averages that yield the most effective energy balance closure are identified as  
31 45 and 60 minutes.
- 32 2. Insufficiently short time-averages such as 1 and 5 minutes, as well as excessively long-  
33 time-averages such as 120 minutes, resulted in a high relative error in representing  
34 carbon and water fluxes.
- 35 3. The conventional 30-minute averaging period proved to be insufficient in capturing  
36 low-frequency fluxes, necessitating the use of longer averaging periods.
- 37 4. Time-averaging of Eddy Covariance fluxes needs to be performed in accordance with  
38 crop growth stage.
- 39

## 40 1.0 INTRODUCTION

41 Water use efficiency (WUE) is an important eco-hydrologic trait relating two important  
42 processes of plant metabolism namely carbon fixation (via photosynthesis) and water  
43 consumption (via transpiration) (Bramley, 2013). The need for achieving food security with  
44 diminishing water resources under changing climate has made WUE as the controlling  
45 parameter in planning and design of irrigation strategies (Tang, 2015). Depending on the scale  
46 of investigation, WUE can be quantified at: i) leaf, ii) plant, iii) ecosystem, or iv) regional  
47 scales (Medrano, 2015). Of these, ecosystem WUE has taken precedence in irrigation and  
48 agronomy due to: i) accurate and reliable measurement using micrometeorological techniques,  
49 ii) ability to evaluate the role of various water conservation techniques on ecosystem  
50 productivity, and iii) understand the relation between carbon and water cycles in response to  
51 changes in climate (Tang, 2015; Tong, 2014).

52 Eddy covariance (EC) is a non-destructive, micrometeorological technique for direct  
53 measurement of water vapour (H<sub>2</sub>O) and carbon (CO<sub>2</sub>) fluxes between vegetation and  
54 atmosphere at high temporal frequency (Aubinet, 1999; Leclerc and Foken, 2014). EC method  
55 precisely measures the overall transfer of heat, mass, and momentum between the earth's  
56 surface (such as vegetation) and the atmosphere. This is achieved by estimating the covariance  
57 of turbulent fluctuations in vertical wind (referred to as eddies) with respect to the specific flux  
58 under consideration such as H<sub>2</sub>O, CO<sub>2</sub>, temperature. EC represents the scalar fluxes of interest  
59 (representative of eco-hydrological processes) from a region upwind of the measurement  
60 known as the footprint. At ecosystem scale, WUE is estimated as the ratio of net primary  
61 product (NPP): proxy for photosynthesis to evapotranspiration (ET): proxy for water



62 consumption (Peddinti, 2020). WUE is a key eco-hydrologic trait that is used to analyse the  
63 role of climate change, drought, deficit irrigation, and management strategies on ecosystem  
64 productivity. Currently, EC is the most accurate and reliable method for estimating carbon and  
65 water fluxes, hence WUE at ecosystem scale (Tong, 2009). A number of studies have  
66 demonstrated the efficacy of EC in estimating WUE across a wide range of ecosystems (Tang,  
67 2015; Tong, 2014; Wang, 2017). Despite improvements in measurement accuracy, data  
68 sampling, and processing techniques, EC method suffers from the drawback of lack of  
69 conservation among the energy terms, resulting in energy balance closure (EBC) problem  
70 (Charuchittipan, 2014; Foken, 2011; Reed, 2018). Lack of EBC as observed in EC system is  
71 reported across diverse ecosystems ranging from simple bare soils (Oncley, 2007), to  
72 homogeneous grasslands (Twine, 2000), to heterogeneous croplands (Peddinti and  
73 Kambhammettu 2019), to complex forest (Charuchittipan, 2014; Wilson, 2002). Apart from  
74 the errors associated with instrumentation, measurement, and neglected energy sinks, lack of  
75 EBC at the EC sites is also attributed to the omission of low frequency secondary circulations  
76 in the turbulent flux estimation (Wilson, 2002). This problem can be circumvented by choosing  
77 appropriate averaging period during flux estimation, the selection of which is based on: i)  
78 ‘ensemble block time-averaging method’ (Finnigan, 2003; Malhi, 2004; Sakai, 2001), and ii)  
79 ‘ogive method’ (Berger, 2001).

80 A number of studies have highlighted the importance of averaging period in quantifying  
81 the EC fluxes, with an objective to obtain optimal time-averaging period under various canopy  
82 and surface roughness conditions. While smaller averaging periods (15-30 min.) are suitable  
83 for managed croplands, flux estimation from forest and tall canopies demand longer averaging  
84 periods (60-120 min.) due to the presence of large-sized, slow moving eddies (Finnigan, 2003;  
85 Sakai, 2001; Sun, 2006). Zhang (2013) concluded that time-averaging of EC fluxes has to be  
86 done in accordance with the observation scale. In an analysis of Chengliu riparian forest in  
87 China, they found that lower time-averaging periods (15 min.) are suitable for daily variation  
88 of EC fluxes, whereas higher time-averaging periods (60 min.) are suitable for long-term flux  
89 computations. A similar observation was made by Lee (2004) over farmlands. In a wheat field  
90 in Yucheng, China, 10 min. and 30 min. averaging periods were found suitable for diurnal and  
91 long-term flux observations respectively. Flux observations over a Maize crop at Daxing  
92 experimental station in China conclude that optimal time-averaging period has to be considered  
93 in accordance with crop growth stage (Feng, 2017). However, they observed a marginal (< 3



94 %) error in representing the fluxes at conventional 30 min. averaging relative to the optimal  
95 averaging obtained for each growth stage.

96 Maize is the third most important cereal crop in India after rice and wheat, and accounts  
97 for about 10 % of total food production in the country (Sharma, 2018; Ficci 2014). In spite of a  
98 huge area under cultivation (9.4 MHa), high production (23 million tons), and enormous water  
99 consumption (18 BCM), both crop productivity (2.5 t ha<sup>-1</sup>) and crop water productivity: CWP  
100 (1.83 kg m<sup>-3</sup>) of Indian Maize are far lower than corresponding world averages (Sharma, 2018).  
101 Low CWP (hence, WUE) of Indian Maize can be attributed to: i) a high dependence (85 %) on  
102 erratic, uncertain rainfall, ii) low adoption of hybrid varieties, iii) improper drainage facilities  
103 leading to water logging, and iv) unscientific application of irrigation water without analysing  
104 soil-water-crop interactions (Shankar, 2012). Thus, an accurate quantification of WUE and its  
105 temporal variation during the crop cycle is essential for effective irrigation water management  
106 of Maize crop (Medrano, 2015).

107 While the effect of time-averaging on carbon and water fluxes measured at EC sites is  
108 reported, the effect on their interaction term, i.e. WUE, which is crucial in irrigation water  
109 management is unexplored. Evaluation of time-averaging period on WUE dynamics is  
110 necessary to understand the contribution of low and high frequency photosynthetic carbon and  
111 evaporative water fluxes generated from various field management strategies. Also, most of  
112 the EC flux studies are confined to data rich AmeriFLUX, EuroFLUX, and ChinaFLUX sites,  
113 with limited focus to Indian fragmented croplands. This motivates the present study, and the  
114 objectives of this study are as follows: i) investigate the role of time-averaging of EC fluxes on  
115 EBR and WUE dynamics, ii) compute optimal averaging period to simulate carbon and water  
116 (hence, WUE) fluxes of Maize crop, and iii) investigate the association of carbon, water, and  
117 WUE fluxes between multiple averaging periods. Results of this study can help in designing  
118 efficient management strategies using EC datasets in response to changes in WUE during the  
119 crop cycle.

120

## 121 **2.0 MATERIALS AND METHODOLOGY**

### 122 **2.1 Site Description and Instrumentation**

123 Controlled Maize plots situated at Professor Jaya Shankar Telangana State Agricultural  
124 University (PJ TSAU), Hyderabad, Telangana, India (17°19'17" N, 78°24'35" E, 559 m above



125 sea level) forms the study area. The region is composed of red gravel to sandy loam soils with  
126 field capacity and wilting point in the ranges of 17.92 - 19.56 % and 8.2 – 9.87% respectively.  
127 As per Koppen-Geiger's classification, the region falls under tropical savanna climate zone  
128 (Aw) characterized by long dry and short wet seasons (Kottek, 2006). Mean annual  
129 precipitation of the region is 900 mm (IMD, 2019) with more than 80% occurring during the  
130 monsoon months (Jun-Sep). Temperatures are high during summer ( $38.33 \pm 2.12$  °C) and low  
131 during winter ( $30 \pm 2.20$  °C) months. Humidity of the region varies from 35% in summer to  
132 73% in monsoon (CGWB, 2013). Mean seasonal wind speed is in the range of 1.5 to 2.7 m/s  
133 (Peddinti and Kambhammettu 2019). Hydro-geologically, the study area forms part of the  
134 Deccan plateau characterized by multiple layers of solidified flood basalt resulting from  
135 volcanic eruptions. Depth to groundwater ranges from 12 m (pre-monsoon) to 6 m (post-  
136 monsoon) (CGWB, 2013).

137 Meteorological parameters and turbulent fluxes were obtained for one crop season, i.e.  
138 26 May to 06 Sep, 2019 using an open path eddy covariance (EC) flux tower. The flux system  
139 is composed of a 3D sonic anemometer (CSAT3, Campbell Sci. Inc., USA), and an open-path  
140 fast response infrared gas analyzer (IRGASON-EB-IC, Campbell Sci. Inc., USA) to measure  
141 CO<sub>2</sub> and H<sub>2</sub>O fluxes at 3 m above the canopy. Raw data was collected with a logger (CR1000,  
142 Campbell Sci. Inc., USA) at 10 Hz frequency. Additionally, slow response meteorological  
143 variables including precipitation (TE525-L-PTL, Tipping Bucket, Campbell Sci. Inc., USA),  
144 soil heat flux (HFP01SC-L-PTL, Campbell Sci. Inc., USA), solar radiation (CNR 4, Campbell  
145 Sci. Inc., USA), and soil moisture (CS616-L-PT-L, Campbell Sci. Inc., USA) were obtained at  
146 10 min. intervals.

147

## 148 2.2 Data Collection and Processing

149 Table 1 shows the phenological stages of the Maize crop in the study area (Soujanya,  
150 2021). Additionally, leaf-area index (LAI) and mean plant height were measured during the  
151 crop cycle (Table 1). The LAI was measured using the plant canopy analyser, whereas the plant  
152 height was measured using a ruler from the base of the plant to its crown. Maize crops of the  
153 experimental fields are sown on 25<sup>th</sup> May 2019 and harvested on 6<sup>th</sup> September 2019 with a  
154 base period of 104 days.

155 **Table 1:** Phenological growth stages and physical properties of the Maize crop



---

S. No.	Growth stage	Start date	End date	Period Length (days)	Leaf Area Index (m <sup>2</sup> m <sup>-2</sup> )	Plant height (cm)
1	6 <sup>th</sup> leaf	26/05/2019	12/06/2019	18	0.61	46.8
2	Silking	13/06/2019	19/07/2019	37	1.56	75.2
3	Dough	20/07/2019	12/08/2019	24	3.46	133
4	Maturity	13/08/2019	06/09/2019	25	3.03	134

---

156

157 Data from the EC system at 10 Hz frequency was converted to ASCII format using  
158 LoggerNet (4.3) software (Campbell Scientific Inc., Logan, Utah, USA), and further  
159 aggregated to various averaging periods (1, 5, 10, 15, 30, 45, 60, and 120 minutes). Post data  
160 processing was done using EddyPro post-processing software (version 7.0.8, LI-COR, USA).  
161 Primary corrections performed on the raw data include tilt corrections, turbulent fluctuations,  
162 density fluctuations, frequency corrections and quality checks. Tilt corrections were made by  
163 the double axis rotation method. The block average method and linear detrending method were  
164 used to correct the turbulent fluctuations. Density fluctuation corrections were done using  
165 Webb–Pearman–Leuning (WPL) method. Quality checks were performed following a flagging  
166 policy proposed by Mauder and Foken (2006) (0-1-2 system). Flag set to "0" corresponds to  
167 the best quality fluxes, "1" corresponds to fluxes acceptable for general analysis, and "2"  
168 corresponds to poor quality fluxes that should be removed from the dataset. The resulting fluxes  
169 may exhibit spikes, discontinuity, randomness etc. There is a need to perform secondary  
170 corrections on the data that include flux spike removal (Vickers and Mahrt 1997), friction  
171 velocity corrections, gap filling and uncertainty analysis (Finkelstein, 2001), skewness &  
172 kurtosis removal, spectral corrections, and frequency corrections. To correct flux estimates for  
173 low and high frequency losses due to instrument setup, intrinsic sampling limits of the devices,  
174 and various data processing decisions, spectral corrections are performed. Additionally, slow  
175 sensor meteorological data obtained at 1 min. interval were processed for different time-  
176 averaging periods using the EddyPro post-processing software (version 7.0.8, LI-COR, USA).

177



178 **2.3 Effect of time-averaging on EBR and EC fluxes**

179 Lack of conservation among the measured energy terms of the EC tower is referred as  
180 energy balance closure (EBC). The available energy ( $R_n-G$ ) is generally higher than the  
181 turbulent fluxes ( $H+LE$ ), resulting in a positive balance (Eshonkulov, 2019) where  $R_n$ ,  $G$ ,  $H$   
182 and  $LE$  correspond to net radiation, soil heat flux, sensible heat and latent heat respectively.  
183 Apart from instrument and measurement issues, this lack of energy closure is thought to be  
184 partly from averaging periods and coordinate systems (Finnigan, 2003; Finnigan, 2004;  
185 Gerken, 2018). The energy closure fraction, commonly termed as energy balance ratio (EBR)  
186 is used to evaluate the quality of EC data by examining energy fluxes at the surface (Chen and  
187 Li 2012), given by:

188 
$$EBR = \frac{H+LE}{R_n-G} \quad (1)$$

189 EBR helps to determine the averaging period required to calculate  $H$  and  $LE$  fluxes over a  
190 range of landscapes (Chen and Li 2012). A high EBR ( $EBR \geq 0.7$ ) ensures reliability of EC  
191 observations for use with flux estimation.

192 Eddy fluxes are computed as the covariance between instantaneous deviation in vertical  
193 wind speed ( $w'$ ) and scalar component of interest ( $s'$ ) from their respective means, given by

194 
$$F \approx \overline{\rho_a w' s'} \quad (2)$$

195 where  $\overline{\rho_a}$  is the mean air density, and the overbar represents the time-average of eddy fluxes,  
196 which is of interest in the present study. Depending on the scalar component considered (ex:  
197 temperature, water vapour ( $H_2O$ ), carbon dioxide ( $CO_2$ ) concentration), corresponding eddy  
198 fluxes (ex: sensible heat, latent heat, carbon flux) are computed as below.

199 
$$F_{CO_2} \approx \overline{\rho_a w' CO_2'} \quad (3)$$

200 
$$F_{H_2O} \approx \overline{\rho_a w' H_2O'} \quad (4)$$

201 Ecosystem WUE is then estimated as the ratio of daytime carbon (net primary product) to water  
202 fluxes (evapotranspiration), observed during daytime unstable atmospheric conditions (08:00  
203 am to 04:00 pm) given by:



$$204 \quad WUE = \frac{NPP}{ET} = \frac{F_{CO_2}}{F_{H_2O}} \quad (5)$$

205 Fluxes originating from real-world sites are composed of both high frequency (turbulence) and  
206 low frequency (advection) fluctuations, with a spectral gap in between. Isolating local  
207 turbulence component for use with flux studies is achieved by choosing an appropriate  
208 averaging period,  $T_1$  (typically 30 minutes) on fast response measurements operating at high  
209 frequency  $T_2$  (Manon and Kristian 2020). Optimal averaging period ( $T_1$ ) should be long enough  
210 to reduce random error (Berger, 2001) and short enough to avoid non-stationarity associated  
211 with advection (Foken & Wichura, 1996). The flux estimates (eq. 2) are further decomposed  
212 into frequency dependent contributions, known as co-spectra  $Co_{ws}(f)$  between vertical wind  
213 velocity ( $w$ ) and scalar of interest ( $s$ ) for frequencies ' $f$ ' (Manon and Kristian 2020). For an  
214 accurate estimation of the flux, it is essential that the EC method is applied under conditions  
215 where the flow is stationary, and all eddies carrying flux are sampled. Given that the flow  
216 remains stationary, an 'ogive' serves as a check for the essential requirement to sample all  
217 scales carrying the flux. Ogive function is well proposed to check if all low frequency fluxes  
218 are included in the turbulent flux measured with the EC method (Foken & Wichura, 1996;  
219 Foken et al., 2005). It is used to investigate the energy balance losses caused by low frequency  
220 fluxes. Ogive analysis is performed to investigate the flux contribution from each frequency  
221 range and to arrive at most suitable averaging period to capture most of the turbulent fluxes  
222 (Desjardans, 1989; Charuchittipan, 2014). Ogive function thus provides the cumulative sum of  
223 co-spectral energy starting from the highest frequency, given by:

$$224 \quad Og_{ws}(f_0) = \int_{f_0}^{\infty} Co_{ws}(f) df \quad (6)$$

225 The point of convergence on the Ogive plot to an asymptote corresponds to optimal averaging  
226 period ( $T_1$ ) for use with averaging of high frequency turbulence fluxes. A total of eight  
227 averaging periods, i.e., 1, 5, 10, 15, 30, 45, 60, and 120 minutes were considered to investigate  
228 the role of time-averaging on EBR and EC fluxes, and further to arrive at the optimum  
229 averaging period for use with WUE estimation. The biophysical and physiological  
230 characteristics such as plant height, crop water requirement, LAI, etc. changes with respect to  
231 the crop growth stage (Chintala et al., 2024) and have a significant effect on the EC fluxes. For  
232 this reason, time-averaging of EC fluxes is separated based on crop growth stage.





## 234 2.4 Performance Evaluation

235 The ability of various averaging periods to close the energy balance and compute the  
236 EC fluxes is evaluated using three goodness of fit indicators, namely: a) coefficient of  
237 determination ( $R^2$ ), b) root mean squared error (RMSE), and c) relative error (RE). While  $R^2$   
238 and RMSE aim to quantify the error in closing the energy balance, RE is aimed to compute the  
239 error in estimating EC fluxes with conventional 30 min. averaging period relative to optimal  
240 averaging period.

241 Root mean square error (RMSE) measures overall accuracy in closing the energy balance for  
242 a given averaging period by penalizing large errors heavily, given by:

$$243 \text{RMSE} = \left[ \frac{\sum_{i=1}^n (R_n - G)_i - (H + LE)_i}{n} \right]^{0.5} \quad (7)$$

244 Where  $n$  is the number of observations.

245 Coefficient of determination ( $R^2$ ) is a measure of the strength of linear association between  
246 turbulent fluxes and available energy, given by:

$$247 R^2 = \left\{ \frac{\sum_{i=1}^n [(R_n - G)_i - \overline{(R_n - G)}] [(H + LE)_i - \overline{(H + LE)}]}{\sqrt{\sum_{i=1}^n [(R_n - G)_i - \overline{(R_n - G)}]^2 [(H + LE)_i - \overline{(H + LE)}]^2}} \right\}^2 \quad (8)$$

248 Relative error (RE) provides the disparity in the fluxes estimated with conventional (30 min.)  
249 relative to the fluxes estimated with optimal averaging period, given by:

$$250 RE = \left[ \frac{F_{opt} - F_{30min}}{F_{opt}} \right] \times 100 \quad (9)$$

251 where  $F_{opt}$  and  $F_{30}$  are the flux of interest considering optimal and conventional (30 min.)  
252 averaging periods.

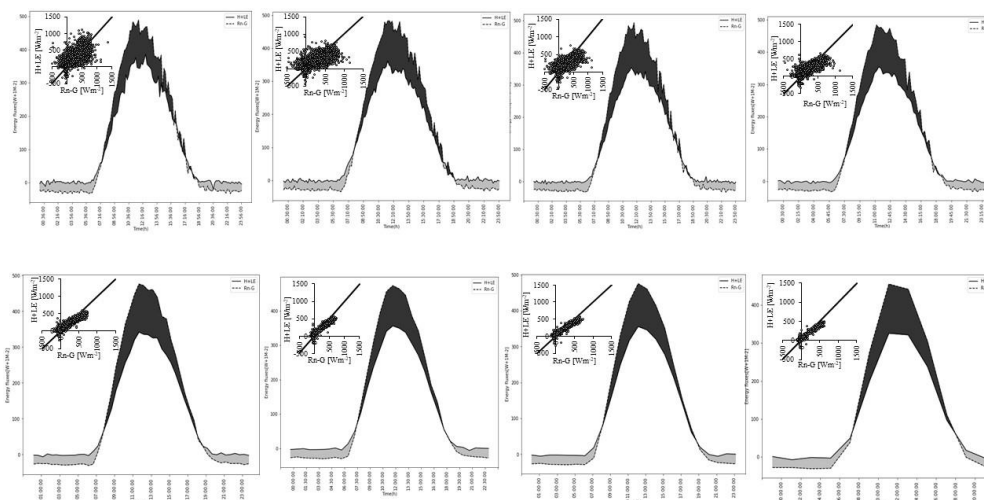
253 A high  $R^2$  (close to 1), low RMSE (close to zero), and low RE (close to zero) is considered to  
254 be the optimal choice in representing the EC fluxes.

255

## 256 3.0 RESULTS AND DISCUSSION

### 257 3.1 Diurnal variations in energy balance components

258 To understand the energy variation in response to rapid changes in meteorological  
259 conditions, we analysed the diurnal variations in energy balance components. Figure 1 shows



260

261 **Figure 1:** Diurnal variations in energy balance components (available energy:  $R_n-G$  and turbulent fluxes:  
262  $H+LE$ ) during the crop cycle with different averaging periods. Inset: Scatter-plots between the two  
263 datasets.

264 the diurnal variations in available energy ( $R_n-G$ ) and turbulent fluxes ( $H+LE$ ) averaged over  
265 the crop cycle for various time-averages. The diurnal variations of ( $R_n-G$ ) and ( $H+LE$ ) are bell-  
266 shaped, with peak occurring at around noon ( $480.16 \pm 14.15 \text{ Wm}^{-2}$ ,  $356.23 \pm 18.51 \text{ Wm}^{-2}$ )  
267 (Figure 1). The energy balance difference (shaded areas of the figure) is found to be positive  
268 ( $76.88 \pm 43.14 \text{ Wm}^{-2}$ ) during daylight hours (08:00 am to 06:00 pm) and is negative ( $-24 \pm$   
269  $11.65 \text{ Wm}^{-2}$ ) for the remaining time. The vertical offset between the two curves, representing  
270 the residual of energy balance is highest around the noon ( $142.39 \pm 19.42 \text{ Wm}^{-2}$ ), and is  
271 consistent between the averaging periods. For an average site-day, the cumulative energy  
272 balance difference was found to be constant with a mean of  $1811 \pm 91.56 \text{ Wm}^{-2}$  at all averaging  
273 periods. The cumulative energy balance difference is crossing the ‘zero’ line at around 11:30  
274 am. The variation is rough at lower averaging periods due to a high sample size ( $n= 10859$  at  
275  $T = 1 \text{ min.}$ ) and is gradually smoothed towards higher averaging periods ( $n= 811$  at  $T = 120$   
276 min.). The slope of regression lines between ( $H+LE$ ) and ( $R_n-G$ ) considering all averaging  
277 periods are in the range of 0.59 to 0.71 with a mean of  $0.65 \pm 0.041$ . The intercept is ranged  
278 from  $19.01$  to  $31.56 \text{ Wm}^{-2}$ . The best slope ( $\geq 0.70$ ) and intercept ( $\leq 20 \text{ Wm}^{-2}$ ) were achieved  
279 with 45 and 60 minutes averaging periods, which is consistent with literature (Gao, 2017;  
280 Leuning, 2012). The strength of linear association between ( $R_n-G$ ) and ( $H+LE$ ) around the best  
281 fit line, explained by  $r$  is high ( $0.80 < r \leq 0.9$ ) at low averaging periods, i.e., 1, 5, 10 minutes,  
282 and is very high ( $r > 0.9$ ) for other averaging periods (Table 2). However, the departure of the



283 data from 1:1 line is relatively low both at low and high averaging periods. Our findings show  
284 that averaging period has minimal influence in representing the energy balance terms.

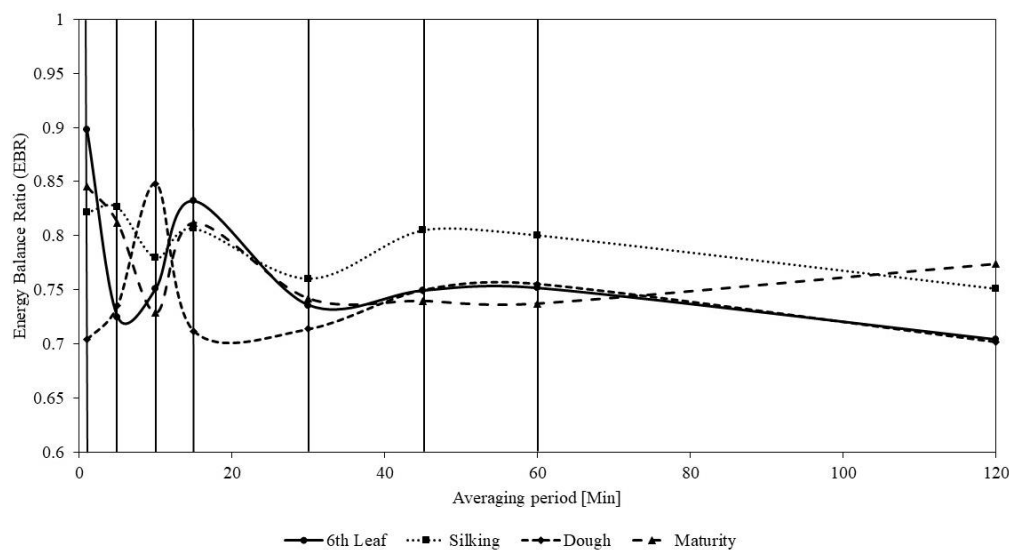
285 **Table 2:** Summary of linear regression parameters in closing the energy balance with different  
286 averaging periods.

Averaging Period	Slope	R <sup>2</sup>	Intercept (Wm <sup>-2</sup> )	r	N	RMSE (Wm <sup>-2</sup> )
1min	0.63	0.66	30.31	0.81	10859	98.38
5min	0.59	0.74	31.56	0.86	10785	76.47
10min	0.60	0.80	28.94	0.90	10753	64.41
15min	0.63	0.84	26.56	0.92	7150	58.18
30min	0.66	0.93	20.49	0.96	3554	38.33
45min	0.70	0.94	19.99	0.97	2355	36.30
60min	0.71	0.94	19.01	0.97	1765	35.07
120min	0.67	0.93	20.77	0.96	811	39.95

287

### 288 3.2 Effect of averaging period on EBR and EC fluxes

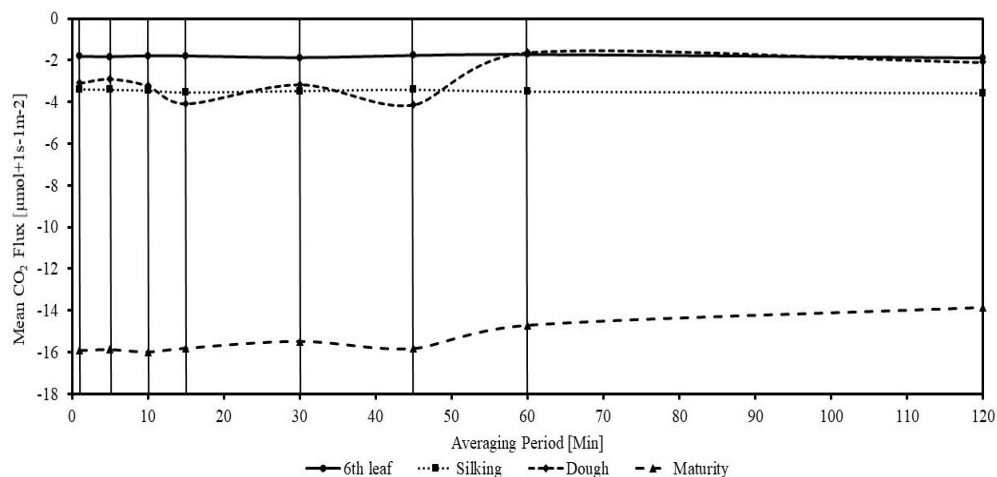
289 The variation in energy balance ratio (EBR) with averaging period for individual  
290 growth stages of the crop is presented in Figure 2. We observed a clear departure of EBR from



291

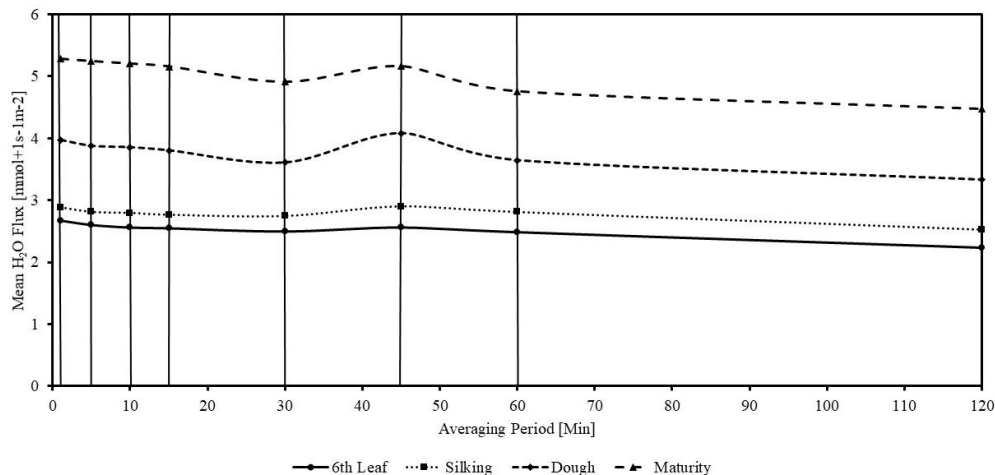
292 **Figure 2:** Variation in energy balance ratio (EBR) with averaging period for different growth stages. (Solid  
293 verticals from left to right correspond to the averaging periods of 1 min., 5 min., 10 min., 15 min., 30 min.,  
294 45 min., 60 min., and 120 min. respectively).

295 unity for all growth stages, particularly with dough and maturity stages due to ignorance of  
296 canopy heat storage. EBR is fluctuating between 0.70 and 0.90 at low (1 – 30 min.) averaging  
297 periods and is fairly constant ( $0.75 \pm 0.03$ ) at high ( $\geq 30$  min.) averaging periods. Our reported  
298 values of EBR during the crop growth are within the typically found range of 0.65 to 1.2 for  
299 most of the crops (Feng, 2017; Finnigan, 2003; Wilson, 2002). The mean EBR with  
300 conventional 30 min. averaging period is found to be 0.74, 0.76, 0.71, and 0.74 during 6<sup>th</sup> leaf,  
301 silking, dough, and maturity stages respectively. Low EBR during the crop cycle can also be  
302 attributed to the ignorance of energy transport associated with large eddies from landscape  
303 heterogeneity, which is not captured by the EC system. Changes in daytime mean carbon and  
304 water fluxes with averaging period for different growth stages of the crop is shown in Figure  
305 3. Carbon fluxes (sink) have a very low mean ( $1.81 \pm 0.06 \mu\text{mol m}^{-2}\text{s}^{-1}$ ) during 6<sup>th</sup> leaf stage,



306

307 **Figure 3a:** Variation in mean carbon fluxes with averaging period for different growth stages (Solid verticals  
 308 from left to right correspond to the averaging periods of 1 min., 5 min., 10 min., 15 min., 30 min., 45 min.,  
 309 60 min., and 120 min. respectively).



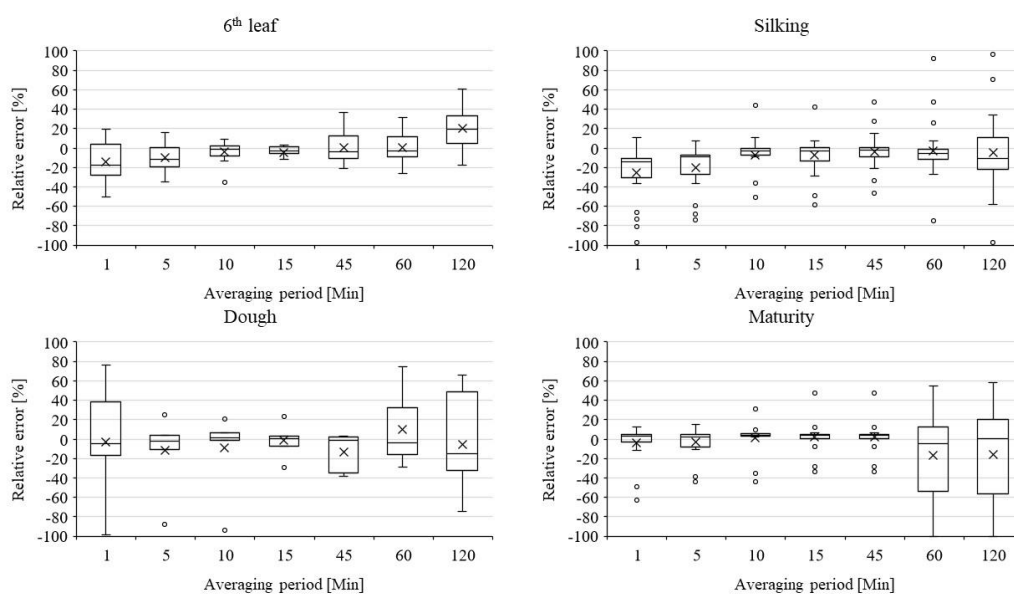
310

311 **Figure 3b:** Variation in mean water fluxes with averaging period for different growth stages (Solid verticals  
 312 from left to right correspond to the averaging periods of 1 min., 5 min., 10 min., 15 min., 30 min., 45 min.,  
 313 60 min., and 120 min. respectively).

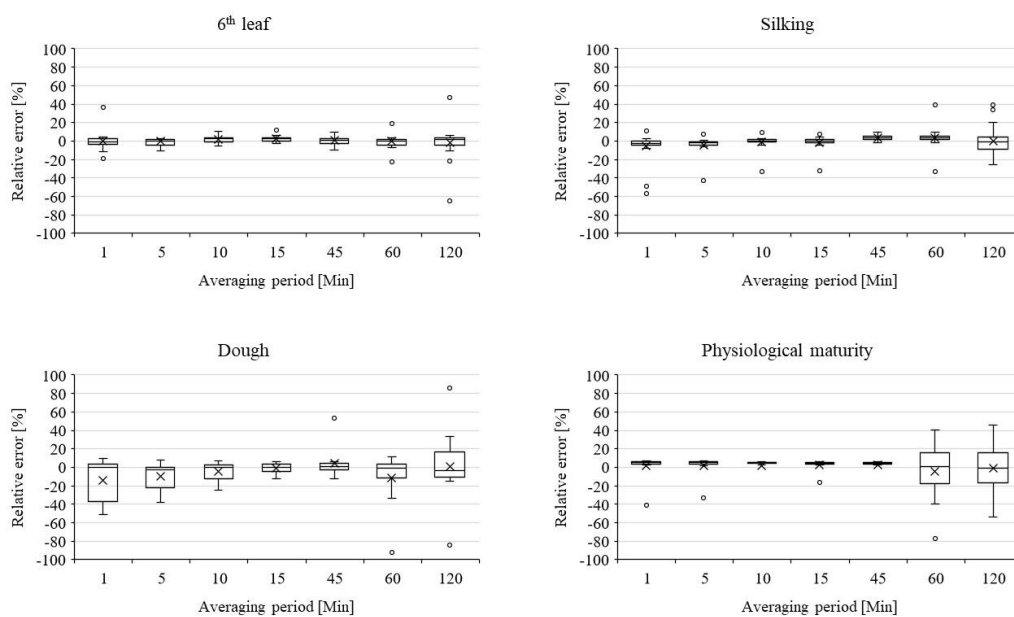
314 low mean during silking ( $3.48 \pm 0.07 \mu\text{mol m}^{-2}\text{s}^{-1}$ ) and dough ( $3.03 \pm 0.87 \mu\text{mol m}^{-2}\text{s}^{-1}$ ) stages,  
 315 and a high mean ( $15.44 \pm 0.75 \mu\text{mol m}^{-2}\text{s}^{-1}$ ) during maturity stage. Mean carbon fluxes during  
 316 6<sup>th</sup> leaf and silking stage are mostly unaffected by averaging period. We observed a gradual  
 317 increase in water vapour fluxes during the crop cycle, from 6<sup>th</sup> leaf ( $2.52 \pm 0.13 \text{ mmol s}^{-1}\text{m}^{-2}$ )  
 318 to maturity ( $5.02 \pm 0.29 \text{ mmol s}^{-1}\text{m}^{-2}$ ). As the averaging period is increased, the mean water  
 319 vapour flux is decreased, with an exception at 45 min. averaging period. Distribution of error



320 in representing carbon and water fluxes at different averaging periods, relative to the  
321 conventional 30 min. averaging period i.e. relative error (RE) is presented in Figure 4. During  
322 6<sup>th</sup> leaf and silking stages, RE in estimating carbon fluxes is high (~ -15 %) with low averaging  
323 periods, and is gradually diminishing towards higher averaging periods, with an exception at  
324 very high (120 min.) average period. For dough and maturity stages, RE is found to be  
325 significant with higher averaging periods (60-120 min). RE in estimating water vapour fluxes  
326 is found to be insignificant at all averaging periods, irrespective of growth stage.



327  
328 **Figure 4a:** Whisker plots showing the distribution of error in estimating carbon fluxes with various  
329 averaging periods relative to the conventional 30 min. averaging.



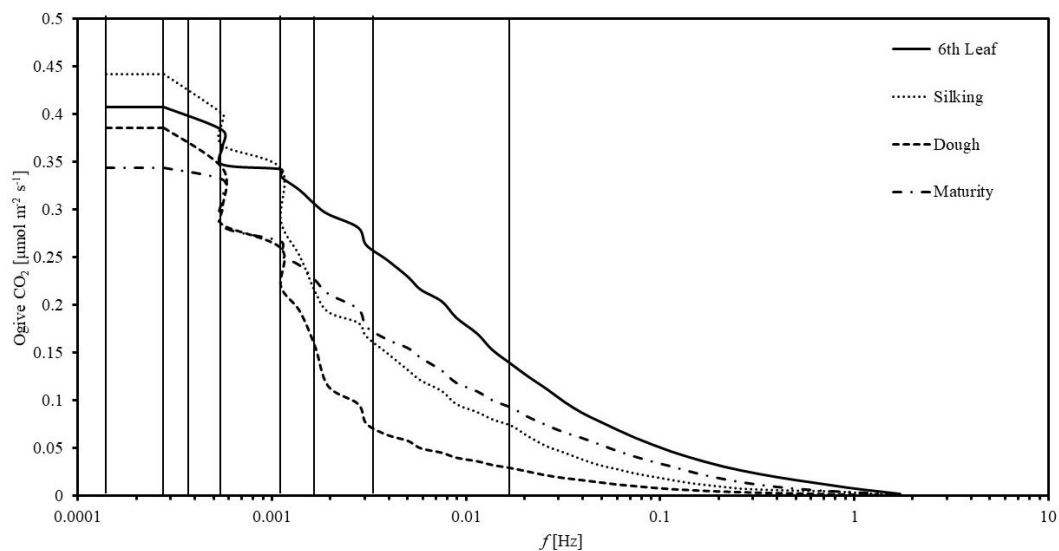
330

331 **Figure 4b:** Whisker plots showing the distribution of error in estimating water fluxes with various averaging  
332 periods relative to the conventional 30 min. averaging.

333

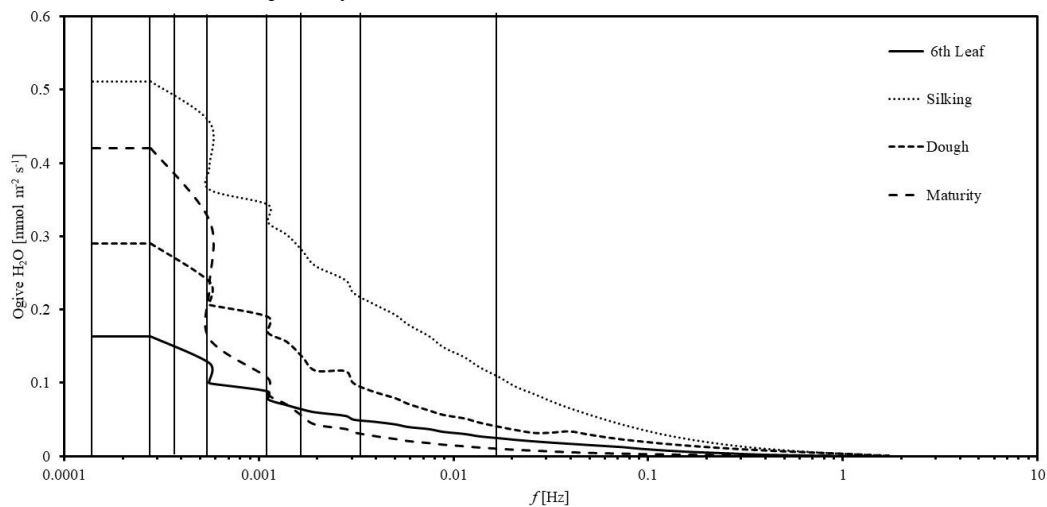
### 334 3.3 Selection of Optimal averaging period

335 Ogive functions representing the cumulative integral of the co-spectral energy starting  
336 with highest frequency, i.e., 0.016 Hz ( $T = 1$  min.) for carbon and water fluxes are presented



337

338 **Figure 5a:** Ogive plots of carbon fluxes for different growth stages of the Maize crop. (Solid verticals from  
339 left to right extremes correspond to the averaging periods of 120 min., 60 min., 45 min., 30 min., 15 min.,  
340 10 min., 5min. and 1 min. respectively).



341

342 **Figure 5b:** Ogive plots of water fluxes for different growth stages of the Maize crop. (Solid verticals from  
343 left to right extremes correspond to the averaging periods of 120 min., 60 min., 45 min., 30 min., 15 min.,  
344 10 min., 5min. and 1 min. respectively)

345 in Figure 5. Shorter time periods corresponding to daytime unstable atmospheric conditions  
346 (08:00 am to 04:00 pm) for various growth stages were investigated. Ogive plots of carbon  
347 fluxes for 6<sup>th</sup> leaf and silking stages showed an increasing trend upto 0.011 Hz (15 min.) and  
348 remained fairly constant before 0.0055 Hz (30 min.). This concludes that whole turbulent  
349 spectrum can be covered with 15 to 30 min. averaging, with negligible flux contribution from  
350 longer frequencies. Ogive plots of carbon fluxes for dough and maturity stages showed a  
351 continuous increasing trend without a defined plateau (horizontal asymptote) in between. This  
352 conclude that the conventional 30 min. averaging period is inadequate to capture the low  
353 frequency fluxes, thus demanding for higher averaging periods. We observed a similar  
354 behaviour with water fluxes (Figure 5). The flat part of the Ogive curve representing the  
355 optimal averaging period was found to vary across the crop cycle. While 15-30 min. time-  
356 average is suitable for aggregating the EC fluxes during 6<sup>th</sup> leaf and silking stages, 45-60 min.  
357 averaging is more appropriate for dough and maturity stages. The crop biophysical factors like  
358 LAI and plant height are minimum during 6<sup>th</sup> leaf and silking stages contributes low quantity  
359 of CO<sub>2</sub> and H<sub>2</sub>O fluxes (refer figure 3a & 3b) whereas they are maximum in the later stages of  
360 the crop i.e., tasselling and maturity contributing to high quantity of CO<sub>2</sub> and H<sub>2</sub>O fluxes (refer  
361 figure 3a & 3b). Our results are in accordance with the previous studies of Fong et al., 2020 on  
362 Cotton, where the responses in NPP and ET were related seasonally to plant growth stages.



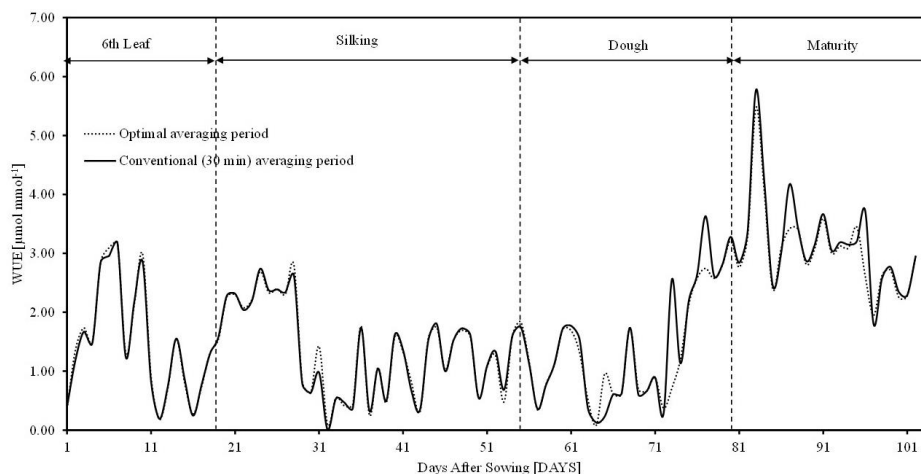


363 The previous studies on various crops revealed that the NPP and ET fluxes were initially low  
364 in the early stages and increases towards maturity stage due to crop phenology and management  
365 practices. To capture these low quantity fluxes, low averaging periods i.e., 15 min. is sufficient,  
366 whereas 45 min. time-averaging period can capture high quantity fluxes that are prevalent  
367 during later growth stages of the crop. As the crop characteristics are dependent on the crop  
368 growth stages, a single time-averaging period is not appropriate to capture the dynamics of CO<sub>2</sub>  
369 and H<sub>2</sub>O fluxes and their ratio WUE. This clearly demonstrates that, as the plant achieves its  
370 higher stage, flux contribution from low-frequency components becomes more valuable. Very  
371 low averaging periods (ex: 1 min., 5 min.) were found unsuitable to capture low-frequency flux  
372 components, which is in agreement with literature (Feng, 2017).

373

#### 374 3.4 Dynamics of Water use efficiency

375 Daily means of water use efficiency (WUE) estimated with conventional 30 min. and  
376 growth specific optimal averaging periods is presented in Figure 6. Mean WUE fluxes for 6<sup>th</sup>



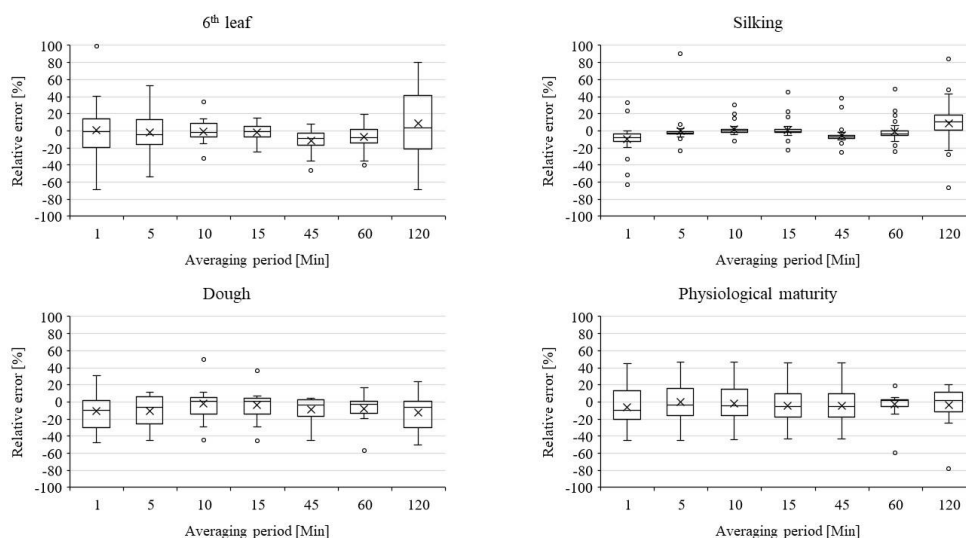
377

378 **Figure 6:** Seasonal variations in daily mean WUE fluxes obtained with conventional 30 min. (black) and  
379 optimal averaging periods (red) during the crop cycle.

380 leaf, silking, dough and maturity stages with conventional 30 min. averaging are  $1.48 \pm 0.96$ ,  
381  $1.36 \pm 0.73$ ,  $1.38 \pm 0.95$  and  $3.184 \pm 0.78$   $\mu\text{mol mmol}^{-1}$  respectively. Corresponding fluxes  
382 with stage specific optimal averaging periods are  $1.49 \pm 0.95$ ,  $1.37 \pm 0.74$ ,  $1.39 \pm 0.79$  and  $3.06$   
383  $\pm 0.69$   $\mu\text{mol mmol}^{-1}$  respectively. Error in estimating mean daily WUE fluxes with 30 min.



384 averaging is very low ( $< 1.45\%$ ) during 6<sup>th</sup> leaf and silking stages, low (8.56 to 9.04 %) during  
385 maturity stage, and is moderate (11.84 to 12.12 %) during dough stage. This conclude that,  
386 choice of optimal averaging period is more crucial for late stage growth periods of the crop.  
387 Distribution of error in estimating WUE fluxes with various averaging periods relative to  
388 conventional 30 min. average period (RE) is presented in Figure 7. A close to zero RE with all  
389 averaging periods during 6<sup>th</sup> leaf and silking stages conclude that, choice of averaging period  
390 has insignificant role in estimating the WUE fluxes, particularly during early growth stages. A  
391 slightly high RE ( $\sim -5.4\%$ ) during dough and maturity stages conclude that, choice of averaging  
392 period matters for WUE estimation during late stage periods. Hence, conventional 30 min.  
393 averaging period can be considered for estimating WUE fluxes during 6<sup>th</sup> leaf and silking  
394 stages, whereas optimal averaging period need to be considered for estimating WUE fluxes  
395 during dough and maturity stages. Correlation charts showing the linear association within  
396 carbon, water, and WUE fluxes represented at different averaging periods is presented in Figure  
397 8. For ease with comparison, data for the entire crop cycle was considered. Linear association

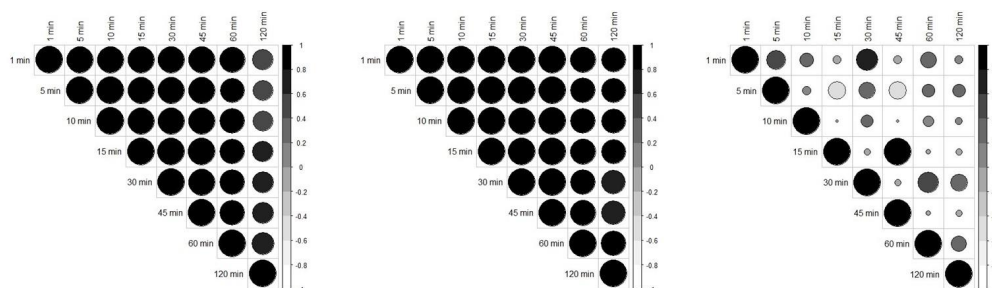


398  
399 **Figure 7:** Whisker plots showing the distribution of error in estimating WUE fluxes with various averaging  
400 periods relative to the conventional 30 min. averaging.

401 between any two averaging periods is positive ( $p > 0.56$ ) for carbon and water fluxes. Except  
402 with 120 min. time-averaging, all other averaging periods are strongly correlated ( $p > 0.87$ )  
403 with 30 min. averaging period. However, a poor linear association in WUE fluxes was observed  
404 between any two averaging periods. This conclude that, the need for optimal averaging period  
405 is more crucial in estimating WUE fluxes rather than individual carbon and water fluxes. Our



406 findings can improve representation of WUE fluxes using EC data, thereby help in developing  
407 efficient water management strategies in response to WUE changes.



408  
409 **Figure 8:** Correlation charts showing the linear association of a) Carbon fluxes, b) Water fluxes, and c)  
410 WUE fluxes estimated with different averaging periods.

411

#### 412 4.0 CONCLUSIONS

413 This study explores the effect of averaging period of EC fluxes on EBR dynamics and  
414 WUE in semi-arid Indian conditions. The proposed methodology was applied on drip-irrigated  
415 maize field for one crop period (May-Sept 2019). Major findings of this study are:

- 416 • EBR was found vary marginally at low averaging periods and less significant during  
417 higher averaging periods.
- 418 • With reference to conventional 30 min. averaging period, relative error is within 12%  
419 for 10-45 min. averaging periods for carbon fluxes and is within 5% for 15-45 averaging  
420 periods for water fluxes.
- 421 • From ogive analysis we found the optimal averaging period as 15 - 30 min. for the 6th  
422 leaf, and silking stages, and as 45 – 60 min. for the dough and maturity stages.
- 423 • The mean carbon fluxes are increasing from  $1.81 \pm 0.06 \mu\text{mol}^+\text{m}^{-2}\text{s}^{-1}$  (6th leaf stage)  
424 to  $15.44 \pm 0.75 \mu\text{mol}^+\text{m}^{-2}\text{s}^{-1}$  (maturity stage) which indicates that carbon sink is a  
425 function of crop growth period. In case of water fluxes, it increased from  $2.52 \pm 0.13$   
426  $\text{mmol}^+\text{m}^{-2}\text{s}^{-1}$  (6th leaf stage) to  $5.02 \pm 0.29 \text{mmol}^+\text{m}^{-2}\text{s}^{-1}$  (maturity stage). Variation of  
427 carbon and water fluxes are directly influencing WUE dynamics.
- 428 • The variation in WUE was increased subsequently with the plant growth and achieved  
429 its maximum value of  $5.17 \mu\text{mol} \text{mmol}^{-1}$  in between dough to maturity stages which  
430 concludes that, crop consumes more carbon than water as the crop period progresses.



431 • The correlation between CO<sub>2</sub> and H<sub>2</sub>O fluxes for all averaging periods was found to be  
432 high. However, WUE, which is calculated as the ratio of CO<sub>2</sub> and H<sub>2</sub>O fluxes, is not  
433 following the same pattern. While 45 min. and 15 min. averaged WUE exhibits a good  
434 correlation, 30 min. averaged WUE is not correlated with other averaging periods.  
435 Averaging period is found to be an influencing factor in controlling WUE, hence should  
436 be considered with caution during the crop growth.

437 This study is limited to understand the role of different time-averaging periods on EC observed  
438 carbon, water fluxes as well as EC derived WUE fluxes. Study findings can help to accurately  
439 characterise WUE of Maize crop considering growth stages for effective implementation of  
440 irrigation strategies.

441

#### 442 **Data Availability Statement:**

443 All footprint climatologies, site-level data files, and supplementary material can be accessed  
444 via the Zenodo Data Repository (<https://zenodo.org/badge/latestdoi/528291820>)  
445 (Shweta07081992, 2022)

446

#### 447 **Author Contribution:**

448 **Arun Rao Karimindla:** Data processing and Analysis, Writing- Original draft. **Shweta**  
449 **Kumari:** Conceptualization, Methodology, Project Supervision. **Saipriya SR:** Data processing  
450 Analysis, and Writing- Original draft. **Syam Chintala:** Data processing and Analysis, Writing-  
451 Original draft. **BVN Phanindra Kambhammettu:** Project Administration, Writing-  
452 Reviewing and Editing.

453

#### 454 **Competing interests:**

455 The authors declare that they have no known competing interests or personal relationships that  
456 could have appeared to influence the work reported in this paper.

457

## 458 **5.0 REFERENCES**

459 Bramley, H., Turner, N. C., & Siddique, K. H. M. (2013). Water Use Efficiency. In C. Kole  
460 (Ed.), Genomics and Breeding for Climate-Resilient Crops: Vol. 2 Target Traits (pp.  
461 225–268). Springer Berlin Heidelberg. [https://doi.org/10.1007/978-3-642-37048-9\\_6](https://doi.org/10.1007/978-3-642-37048-9_6)



- 462 Berger, B. W., Davis, K. J., Yi, C., Bakwin, P. S., & Zhao, C. L. (2001). Long-term carbon  
463 dioxide fluxes from a very tall tower in a northern forest: Flux measurement  
464 methodology. *Journal of Atmospheric and Oceanic Technology*, 18(4), 529–542.
- 465 Central Ground Water Board. (2015). Annual Report 2013.  
466 [https://cgwb.gov.in/old\\_website/Annual-Reports/Annual-Report-2013-14.pdf](https://cgwb.gov.in/old_website/Annual-Reports/Annual-Report-2013-14.pdf)
- 467 Charuchittipan, D., W. Babel, M. Mauder, J. P. Leps, and T. Foken, 2014: Extension of the  
468 Averaging Time in Eddy-Covariance Measurements and Its Effect on the Energy  
469 Balance Closure. *Boundary-Layer Meteorol.*, **152**, 303–327,  
470 <https://doi.org/10.1007/s10546-014-9922-6>.
- 471 Chen, Y. Y., and M. H. Li, 2012: Determining adequate averaging periods and reference  
472 coordinates for eddy covariance measurements of surface heat and water vapor fluxes  
473 over mountainous terrain. *Terr. Atmos. Ocean. Sci.*, **23**, 685–701,  
474 [https://doi.org/10.3319/TAO.2012.05.02.01\(Hy\)](https://doi.org/10.3319/TAO.2012.05.02.01(Hy)).
- 475 Chintala, S., Karimindla, A. R., & Kambhammettu, B. V. N. P. (2024). Scaling relations  
476 between leaf and plant water use efficiencies in rainfed Cotton. *Agricultural Water  
477 Management*, 292, 108680. <https://doi.org/10.1016/j.agwat.2024.108680>
- 478 Desjardins, R. L., MacPherson, J. I., Schuepp, P. H., & Karanja, F. (1989). An evaluation of  
479 aircraft flux measurements of CO<sub>2</sub>, water vapor and sensible heat. *Boundary-Layer  
480 Meteorology*, 47(1), 55–69. <https://doi.org/10.1007/BF00122322>
- 481 Eshonkulov, R., and Coauthors, 2019: Evaluating multi-year, multi-site data on the energy  
482 balance closure of eddy-covariance flux measurements at cropland sites in southwestern  
483 Germany. *Biogeosciences*, **16**, 521–540, <https://doi.org/10.5194/bg-16-521-2019>.
- 484 Feng, J., B. Zhang, Z. Wei, and D. Xu, 2017: Effects of Averaging Period on Energy Fluxes  
485 and the Energy-Balance Ratio as Measured with an Eddy-Covariance System.  
486 *Boundary-Layer Meteorol.*, **165**, 545–551, <https://doi.org/10.1007/s10546-017-0284-8>.
- 487 Ficci, 2014: Maize in India. *India Maize Summit '14*, 1–32.
- 488 Finkelstein, P. L., T. Park, N. Carolina, and F. Sims, 2001:  $z [(w' O') Fc]$ . **106**, 3503–3509.
- 489 Finnigan, J. J., 2004: A re-evaluation of long-term flux measurement techniques part II:  
490 Coordinate systems. *Boundary-Layer Meteorol.*, **113**, 1–41,  
491 <https://doi.org/10.1023/B:BOUN.0000037348.64252.45>.



- 492 Finnigan, J. J., R. Clement, Y. Malhi, R. Leuning, and H. A. Cleugh, 2003: Re-evaluation of  
493 long-term flux measurement techniques. Part I: Averaging and coordinate rotation.  
494 *Boundary-Layer Meteorol.*, **107**, 1–48, <https://doi.org/10.1023/A:1021554900225>.
- 495 Foken, T., and B. Wichura, 1996: Tools for quality assessment of surface-based flux  
496 measurements. *Agric. For. Meteorol.*, **78**, 83–105, [https://doi.org/10.1016/0168-](https://doi.org/10.1016/0168-1923(95)02248-1)  
497 [1923\(95\)02248-1](https://doi.org/10.1016/0168-1923(95)02248-1).
- 498 Foken, T., Göckede, M., Mauder, M., Mahrt, L., Amiro, B., & Munger, W. (2005). Post-  
499 Field Data Quality Control BT - Handbook of Micrometeorology: A Guide for Surface  
500 Flux Measurement and Analysis (X. Lee, W. Massman, & B. Law, Eds.; pp. 181–208).  
501 Springer Netherlands. [https://doi.org/10.1007/1-4020-2265-4\\_9](https://doi.org/10.1007/1-4020-2265-4_9)
- 502 Foken, T., M. Aubinet, J. J. Finnigan, M. Y. Leclerc, M. Mauder, and K. T. Paw U, 2011:  
503 Results of a panel discussion about the energy balance closure correction for trace gases.  
504 *Bull. Am. Meteorol. Soc.*, **92**, <https://doi.org/10.1175/2011BAMS3130.1>.
- 505 Fong, B. N., Reba, M. L., Teague, T. G., Runkle, B. R. K., & Suvočarev, K. (2020). Eddy  
506 covariance measurements of carbon dioxide and water fluxes in US mid-south cotton  
507 production. *Agriculture, Ecosystems and Environment*, 292.  
508 <https://doi.org/10.1016/j.agee.2019.106813>
- 509 Gao, Z., H. Liu, G. G. Katul, and T. Foken, 2017: Non-closure of the surface energy balance  
510 explained by phase difference between vertical velocity and scalars of large atmospheric  
511 eddies. *Environ. Res. Lett.*, **12**, <https://doi.org/10.1088/1748-9326/aa625b>.
- 512 Gerken, T., and Coauthors, 2018: Investigating the mechanisms responsible for the lack of  
513 surface energy balance closure in a central Amazonian tropical rainforest. *Agric. For.*  
514 *Meteorol.*, **255**, 92–103, <https://doi.org/10.1016/j.agrformet.2017.03.023>.
- 515 Kole, C., 2013: *Genomics and breeding for climate-resilient crops: Vol. 2 target traits*. 1–474  
516 pp.
- 517 Kotték, M., J. Grieser, C. Beck, B. Rudolf, and F. Rubel, 2006: World map of the Köppen-  
518 Geiger climate classification updated. *Meteorol. Zeitschrift*, **15**, 259–263,  
519 <https://doi.org/10.1127/0941-2948/2006/0130>.
- 520 Leclerc, M. Y., and T. Foken, 2014: *Footprints in micrometeorology and ecology*. Springer.,
- 521 Lee, X., Q. Yu, X. Sun, J. Liu, Q. Min, Y. Liu, and X. Zhang, 2004: Micrometeorological



- 522 fluxes under the influence of regional and local advection: A revisit. *Agric. For.*  
523 *Meteorol.*, **122**, 111–124, <https://doi.org/10.1016/j.agrformet.2003.02.001>.
- 524 Leuning, R., E. van Gorsel, W. J. Massman, and P. R. Isaac, 2012: Reflections on the surface  
525 energy imbalance problem. *Agric. For. Meteorol.*, **156**, 65–74,  
526 <https://doi.org/10.1016/j.agrformet.2011.12.002>.
- 527 Malhi, Y., K. McNaughton, and C. Von Randow, 2004: Low Frequency Atmospheric  
528 Transport and Surface Flux Measurements. 101–118, [https://doi.org/10.1007/1-4020-](https://doi.org/10.1007/1-4020-2265-4_5)  
529 [2265-4\\_5](https://doi.org/10.1007/1-4020-2265-4_5).
- 530 Manon, M., and M. Kristian, 2020: Estimating local atmosphere-surface fluxes using eddy  
531 covariance and numerical Ogive optimization. **15**, 21387–21432,  
532 <https://doi.org/10.5194/acpd-14-21387-2014>.
- 533 Mauder, M., and T. Foken, 2006: Impact of post-field data processing on eddy covariance  
534 flux estimates and energy balance closure. *Meteorol. Zeitschrift*, **15**, 597–609,  
535 <https://doi.org/10.1127/0941-2948/2006/0167>.
- 536 Medrano, H., and Coauthors, 2015: From leaf to whole-plant water use efficiency (WUE) in  
537 complex canopies: Limitations of leaf WUE as a selection target. *Crop J.*, **3**, 220–228,  
538 <https://doi.org/10.1016/j.cj.2015.04.002>.
- 539 Oncley, S. P., and Coauthors, 2007: The energy balance experiment EBEX-2000. Part I:  
540 Overview and energy balance. *Boundary-Layer Meteorol.*, **123**, 1–28,  
541 <https://doi.org/10.1007/s10546-007-9161-1>.
- 542 Peddinti, S. R., and B. P. Kambhammettu, 2019: Dynamics of crop coefficients for citrus  
543 orchards of central India using water balance and eddy covariance flux partition  
544 techniques. *Agric. Water Manag.*, **212**, 68–77,  
545 <https://doi.org/10.1016/j.agwat.2018.08.027>.
- 546 Peddinti, S. R., Kambhammettu, B. V. N. P., Rodda, S. R., Thumaty, K. C., & Suradhaniwar,  
547 S. (2020). Dynamics of Ecosystem Water Use Efficiency in Citrus Orchards of Central  
548 India Using Eddy Covariance and Landsat Measurements. *Ecosystems*, 23(3), 511–528.  
549 <https://doi.org/10.1007/s10021-019-00416-3>
- 550 Reed, D. E., J. M. Frank, B. E. Ewers, and A. R. Desai, 2018: Time dependency of eddy  
551 covariance site energy balance. *Agric. For. Meteorol.*, **249**, 467–478,





- 552 <https://doi.org/10.1016/j.agrformet.2017.08.008>.
- 553 Sakai, R. K., D. R. Fitzjarrald, and K. E. Moore, 2001: Importance of low-frequency  
554 contributions to eddy fluxes observed over rough surfaces. *J. Appl. Meteorol.*, **40**, 2178–  
555 2192, [https://doi.org/10.1175/1520-0450\(2001\)040<2178:IOLFCT>2.0.CO;2](https://doi.org/10.1175/1520-0450(2001)040<2178:IOLFCT>2.0.CO;2).
- 556 Sharma, B. R., Gulati, Mohan, Gayathri, Manchanda, S., Ray, I., & Amarasinghe, U. (2018).  
557 Water Productivity Mapping of Major Indian Crops. NABARD and ICRIER, 4(1), 88–  
558 100.
- 559 Shankar, V., C. S. P. Ojha, and K. S. H. Prasad, 2012: Irrigation Scheduling for Maize and  
560 Indian-mustard based on Daily Crop Water Requirement in a Semi- Arid Region. **6**,  
561 476–485.
- 562 Soujanya, B., B. B. Naik, M. U. Devi, T. L. Neelima, and A. Biswal, 2021: Dry Matter  
563 Production and Nitrogen Uptake as Influenced by Irrigation and Nitrogen Levels in  
564 Maize. *Int. J. Environ. Clim. Chang.*, 155–161,  
565 <https://doi.org/10.9734/ijecc/2021/v11i1130528>.
- 566 Sun, X. M., Z. L. Zhu, X. F. Wen, G. F. Yuan, and G. R. Yu, 2006: The impact of averaging  
567 period on eddy fluxes observed at ChinaFLUX sites. *Agric. For. Meteorol.*, **137**, 188–  
568 193, <https://doi.org/10.1016/j.agrformet.2006.02.012>.
- 569 Tang, X., Z. Ding, H. Li, X. Li, J. Luo, J. Xie, and D. Chen, 2015: Characterizing ecosystem  
570 water-use efficiency of croplands with eddy covariance measurements and MODIS  
571 products. *Ecol. Eng.*, **85**, 212–217, <https://doi.org/10.1016/j.ecoleng.2015.09.078>.
- 572 Tong, X., J. Zhang, P. Meng, J. Li, and N. Zheng, 2014: Ecosystem water use efficiency in a  
573 warm-temperate mixed plantation in the North China. *J. Hydrol.*, **512**, 221–228,  
574 <https://doi.org/10.1016/j.jhydrol.2014.02.042>.
- 575 Tong, X. J., J. Li, Q. Yu, and Z. Qin, 2009: Ecosystem water use efficiency in an irrigated  
576 cropland in the North China Plain. *J. Hydrol.*, **374**, 329–337,  
577 <https://doi.org/10.1016/j.jhydrol.2009.06.030>.
- 578 Twine, T. E., and Coauthors, 2000: Correcting eddy-covariance flux underestimates over a  
579 grassland. *Agric. For. Meteorol.*, **103**, 279–300, [https://doi.org/10.1016/S0168-  
580 1923\(00\)00123-4](https://doi.org/10.1016/S0168-1923(00)00123-4).
- 581 Vickers, D., and L. Mahrt, 1997: graphDBSummary. *J. Atmos. Ocean. Technol.*, **14**, 512–





- 582           526.
- 583   Wang, X., C. Wang, and B. Bond-Lamberty, 2017: Quantifying and reducing the differences  
584           in forest CO<sub>2</sub>-fluxes estimated by eddy covariance, biometric and chamber methods: A  
585           global synthesis. *Agric. For. Meteorol.*, **247**, 93–103,  
586           <https://doi.org/10.1016/j.agrformet.2017.07.023>.
- 587   Wilson, K., E. Falge, M. Aubinet, and D. Baldocchi, 2002: DigitalCommons @ University of  
588           Nebraska - Lincoln Energy Balance Closure at FLUXNET Sites. *Agric. For. Meteorol.*,  
589           223–243.
- 590   Zhang, P., G. Yuan, and Z. Zhu, 2013: Determination of the averaging period of eddy  
591           covariance measurement and its influences on the calculation of fluxes in desert riparian  
592           forest. *Arid L. Geogr.*, **36**, 401–407.
- 593
- 594